BEILSTEIN JOURNAL OF ORGANIC CHEMISTRY

Synthesis and photorearrangements of 3-acyl-2-hetarylchromones and their spin-labelled derivatives

Mikhail M. Krayushkin, Evgeny V. Tretyakov and Vladimir N. Yarovenko*

Review

Open Access

Address:
N. D. Zelinsky Institute of Organic Chemistry, Russian Academy of Sciences, Leninsky Ave. 47, 119991 Moscow, Russian Federation

Email:
Vladimir N. Yarovenko* - yarovladimir@yandex.ru

* Corresponding author

Keywords:
3-acyl-2-hetarylchromones; fluorescence; optical memory; photorearrangements; spin-labelled compounds

Beilstein J. Org. Chem. **2026,** *22,* 1689–1708.
https://doi.org/10.3762/bjoc.22.137

Received: 27 August 2026
Accepted: 05 November 2026
Published: 18 November 2026

Associate Editor: D. Y.-K. Chen

© 2026 Krayushkin et al.; licensee Beilstein-Institut.
License and terms: see end of document.

Abstract

The paper describes light-sensitive compounds based on 3-acyl-2-hetarylchromones, which undergo irreversible transformation under UV irradiation from a non-luminescent initial form into a stable luminescent one. This photorearrangement process is promising for use in recording media for three-dimensional archival optical memory and photonic photo-controlled devices. The review further addresses the synthesis and characterization of hybrid chromones that combine photoinduced moieties with spin-labelled substituents. A systematic study of such compounds lays the foundation for an emerging interdisciplinary field bridging photochemistry of chromones and molecular magnetism. Advances in this area open prospects for developing new functional materials applicable in fundamental research and industrial technologies.

Introduction

Chromones, as representatives of the benzopyran structure, possess a unique set of properties [1] that enable their versatile application and the design of diverse functional products [2-5]. One particularly attractive feature of chromones is their pronounced light sensitivity and propensity to undergo various photoinduced processes, which are exploited in the development of fluorescent labels for biochemical experiments [6-8].

The rapid development of information technologies necessitates higher data processing speeds and increased storage capacity. The quest for greater data density has driven innovations in optical data storage [9]. For archival optical memory components, there is a demand for compounds that are non-fluorescent in their initial state but can irreversibly rearrange into products exhibiting photoinduced fluorescence [10]. One promising approach involves using compounds containing the photosensitive (*Z*)-3-(2-furyl)- or (*Z*)-3-(2-thienyl)-1-arylpropenone moieties [F(T)AP], which transform under light into a species with induced fluorescence. Various F(T)AP-containing systems have been synthesized, including cyclopentenes **1** [11], benzofurans **2** [12], benzothiopyrans **3** [13], and 3-acyl-2-hetarylchromones **4** [14] (Figure 1).

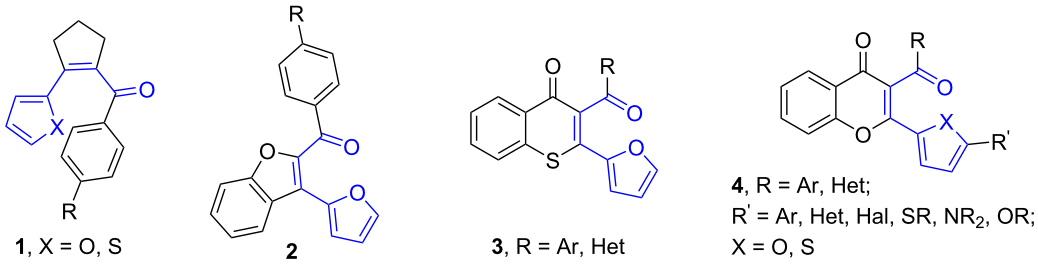
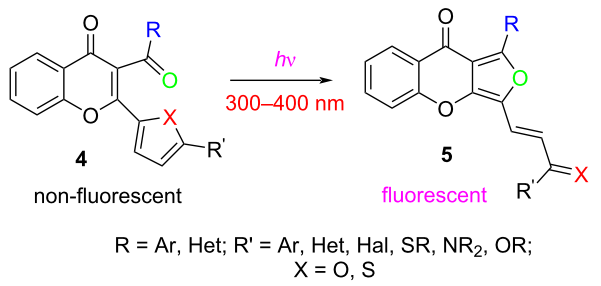


Figure 1: Compounds forming fluorescent products upon UV irradiation.

Among these, the most extensively studied are non-fluorescent chromone derivatives **4** bearing various substituents, which convert under UV irradiation into fluorescent products **5** [15] (Scheme 1). On the basis of 3-acyl-2-hetarylchromones, light-sensitive recording media have been developed, and multilayer optical discs for high-density archival data recording have been fabricated [10,16].



Scheme 1: Formation of fluorescent product **5** from chromone **4** under UV irradiation.

Given the broad spectrum of useful properties of chromones, it appeared promising to design underexplored hybrid products incorporating stable radicals. Advances in the chemistry of stable organic radicals have led to a wide range of functional paramagnetic materials [17-20] with applications in magnetic resonance imaging [21,22], optoelectronics [23], dynamic nuclear polarization as polarizing agents [24], luminescent materials [25], battery components [26,27], molecular spintronic devices [28-30], and high-temperature qubits for quantum technologies [31]. Stable radicals are also widely used in chemical biology and medicine [32-34], e.g., for studying conformational changes in DNA [35], as spin labels for protein structure determination [36,37], in infrared phototheranostics [38], for detecting reactive oxygen species [39], and as novel antioxidants [40,41]; they also show notable antitumor activity [42,43].

Hybrids combining a chromone scaffold with nitroxide or nitronyl nitroxide radicals merge the structural versatility and bioactivity of chromones with the redox and magnetic properties of stable radicals. This synergy offers promising opportunities for advanced materials science and multifunctional molecular systems. A particularly promising direction is the deliberate design of functional systems containing both a paramagnetic group and a fluorophore [44,45]. Integrating chromone structures with nitroxide or nitronyl nitroxide radicals allows one to probe how the paramagnetic moiety influences the photochemistry of chromones.

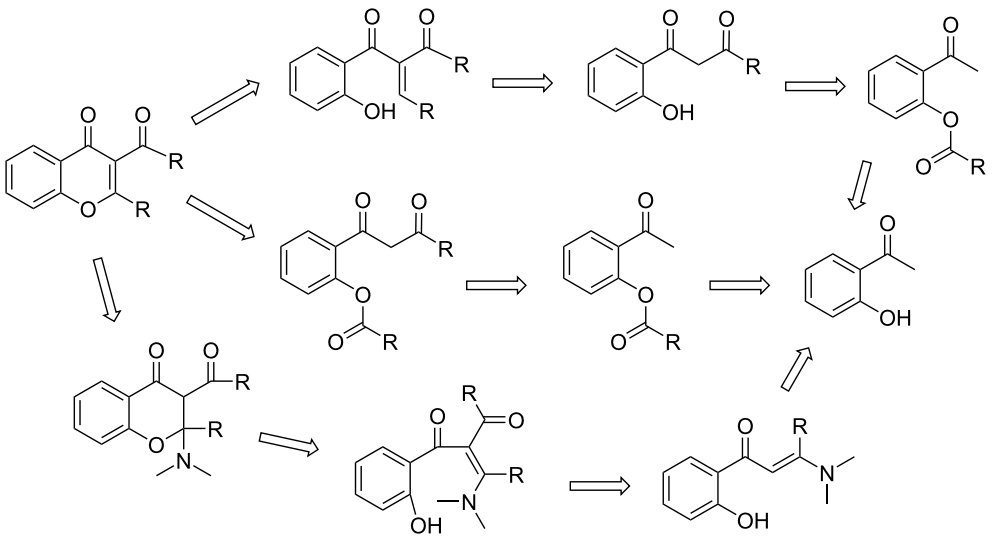
This review summarizes the synthesis, photochemical behavior, and applications of 3-acyl-2-hetarylchromones bearing F(T)AP motifs, with particular emphasis on spin-labelled derivatives. By focusing on this specific chemical space, we aim to provide a coherent picture of a rapidly developing niche that bridges photochemistry, molecular magnetism, and stimuli-responsive materials.

Review

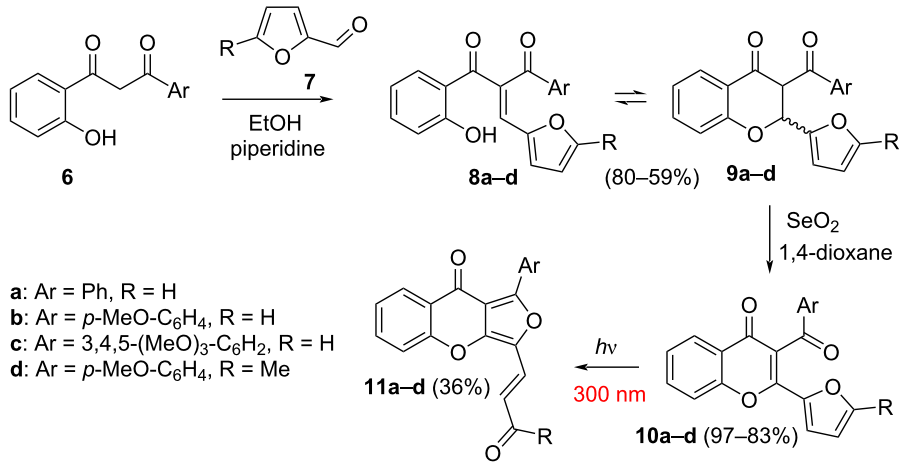
Methods for the synthesis of 3-acyl-2-hetarylchromones

Synthetic approaches to chromone derivatives have been thoroughly reviewed [46,47]. The most widely used method for obtaining 2,3-disubstituted chromones is based on 2-hydroxyaryl ketones [48]. Over the past few decades, notable progress has been achieved in constructing 2,3-disubstituted chromone frameworks from β-ketoenaminones, which are derived from *o*-hydroxyaryl ketones [49] (Scheme 2).

In the 1970s, researchers first reported a series of chromones **10a–d** that exhibited photoactivity, along with the induced fluorescence of their photorearranged products **11a–d** [50]. Scheme 3 illustrates the synthesis of benzopyranones **10a–d** from diketones **6**. In the first step, diketone **6** is refluxed with furfurals **7** in ethanol in the presence of piperidine, yielding intermediates **8a–d** and **9b–d**, which are isolated as one of two isomeric forms. In the subsequent step, oxidation with selenium dioxide in dioxane gives the target



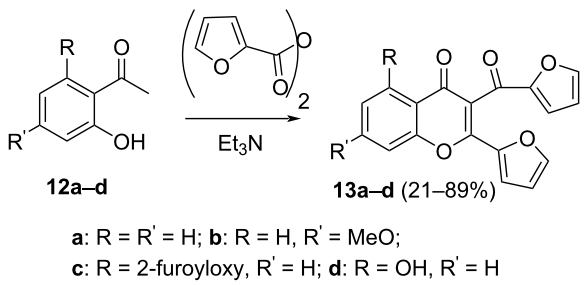
Scheme 2: Retrosynthetic analysis of the structure of 3-acyl-2-arylchromones.



Scheme 3: Synthesis of 3-aroyl-2-furylchromones **10a–d** and their photoinduced rearrangement into compounds **11a–d**.

3-aroyl-2-furylchromones **10a**–**d**. However, only a limited number of products were obtained in this series, and chromones featuring heterocyclic moieties other than furan at the 2-position, as well as those with heterocycles in the acetyl group, were not described.

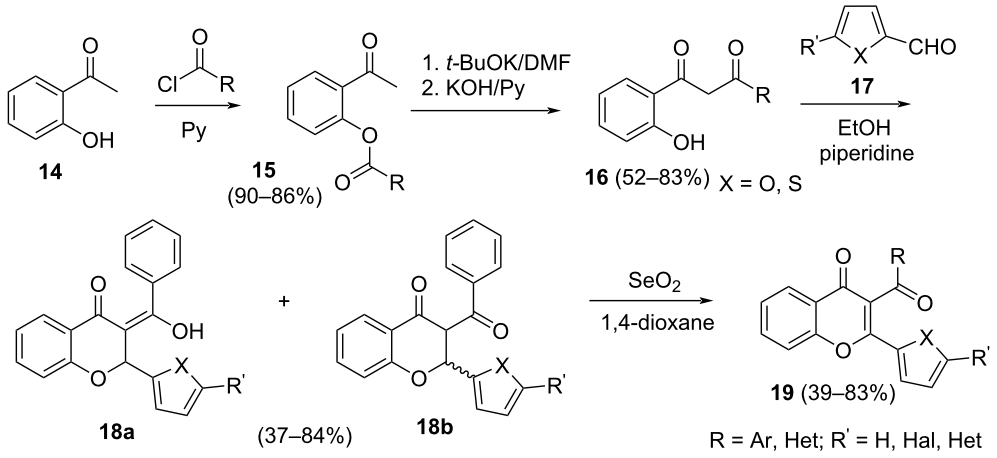
An alternative approach to 3-acyl-2-hetarylchromones involves refluxing 2-hydroxyacetophenones **12a**–**d** in a mixture of 2-furoic anhydride and triethylamine as a base (Scheme 4) [50]. A clear limitation of this method is that it yields only 3-acyl-2-hetarylchromones with identical substituents in the acyl (aroyl) and hetaryl residues. Compounds **13a**–**d** were obtained in yields ranging from 21 to 89%.



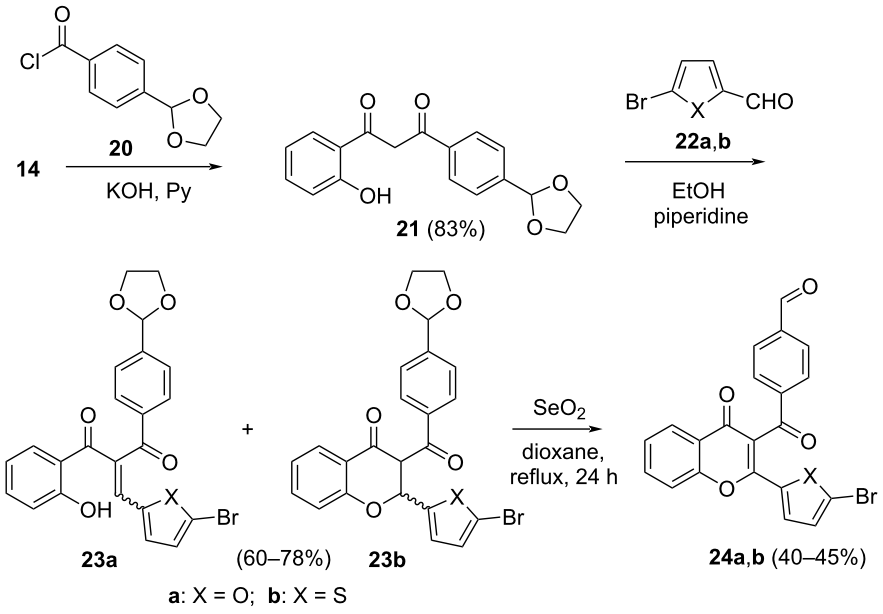
Scheme 4: Synthesis of 3-acyl-2-hetarylchromones **13a–d** using 2-furoic anhydride.

More versatile synthetic strategies were later developed, enabling the preparation of a broad range of photosensitive 3-acyl-2-hetarylchromones **19** (Scheme 5). These compounds are notable for their irreversible photorearrangement into fluorescent species [14]. The synthesis begins with the acylation of *o*-hydroxyacetophenone **14** using acid chlorides of aromatic and heteroaromatic carboxylic acids in anhydrous pyridine, yielding a series of esters **15**. These intermediates then undergo rearrangement – either with *tert*-butoxide in DMF or with KOH in pyridine – to afford species **16**. Subsequently, compounds **16** react with furan-2-carbaldehyde or thiophene-2-carbaldehyde **17** in ethanol. Temperature control (−10 °C to 25 °C) is critical at this stage, with the exact value dictated by the aldehyde's reactivity. A notable trend is the substantial drop in yield when the thiophene unit replaces the furan moiety during the crotonic condensation. The products exist predominantly as tautomeric mixtures **18a**/**18b**, with separability depending on the substitution pattern. The final oxidative step with SeO_2 in dioxane affords the desired 3-aroyl-2-furyl(2-thienyl)chromones **19**, completing the synthetic route.

The synthesis of 4-(2-(5-bromofuryl)-4-oxo-4*H*-chromen-3-carbonyl)benzaldehyde **24a** [51] and 4-(2-(5-bromothienyl)-4-oxo-4*H*-chromen-3-carbonyl)benzaldehyde **24b** [52] has also been reported (Scheme 6). This synthetic route comprises several key steps. First, hydroxyacetophenone **14** reacts with 4-(1,3-dioxo-



Scheme 5: Synthesis of a broad series of 3-acyl-2-hetarylchromones **19**.



Scheme 6: Synthesis of formylchromones **24a**,**b**.

lan-2-yl)benzoyl chloride **20**. The resulting *O*-acylation intermediate then undergoes rearrangement to yield diketone **21**. Next, this diketone is condensed with the corresponding furan- and thiophene-derived aldehydes **22a**,**b** to give a mixture of intermediates **23a** and **23b**. Then the interaction of these intermediates with SeO_2 in dioxane leads to formation of chromones **24a**,**b** with the deprotected aldehyde group.

Modification of photochromic 3-acyl-2-hetarylchromones

A powerful strategy to increase structural diversity in the 3-acyl-2-hetarylchromone family involves the modification of hydroxyacetophenone-derived chromone scaffolds. This approach unlocks a broader range of functionalized derivatives with tailored photophysical properties. A representative example is the nucleophilic displacement of bromine in 3-acyl-2-(5-bromofuryl)chromones and 3-acyl-2-(5-bromomethylfuryl)chromones using *N*-, *S*-, and *O*-nucleophiles (Scheme 7) [53]. The high reactivity of the bromo substituent in **25a**–**c** stems from its activation by the electron-withdrawing chromone moiety. Consequently, the substitution can be performed under mild conditions in ethanol or, alternatively, under thermal activation in DMF. Notably, the reaction may proceed with K_2CO_3 or, depending on the nucleophile, even in the absence of a base, underscoring the versatility of this transformation.

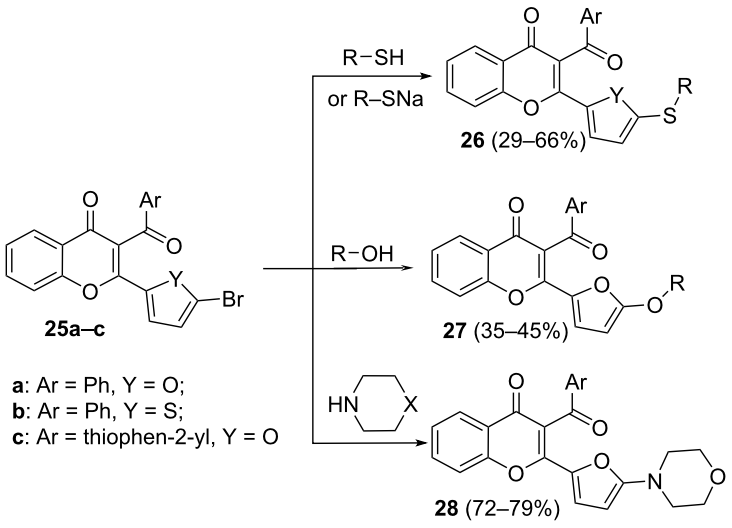
Derivatives bearing bromomethyl groups on the furan or thiophene rings **30a**,**b** have been synthesized. Building on these compounds, researchers obtained chromone derivatives **31**–**33**, in which the heterocycle is linked to amino, thio, or oxo groups via a methylene spacer (Scheme 8) [53].

Chromones containing benzene rings with a bromomethyl group in the acyl moiety **34** were obtained by benzylic bromination of the corresponding methyl derivatives. These substrates readily undergo nucleophilic substitution with *S*-, *N*-, and *O*-nucleophiles to afford the corresponding products **35a**–**e** (Scheme 9) [54]. It is important to note that nucleophilic reactions of 3-acyl chromones may initiate cascade rearrangements, potentially leading to the formation of various heterocyclic products [55]. This side pathway must be considered when designing transformations based on this scaffold.

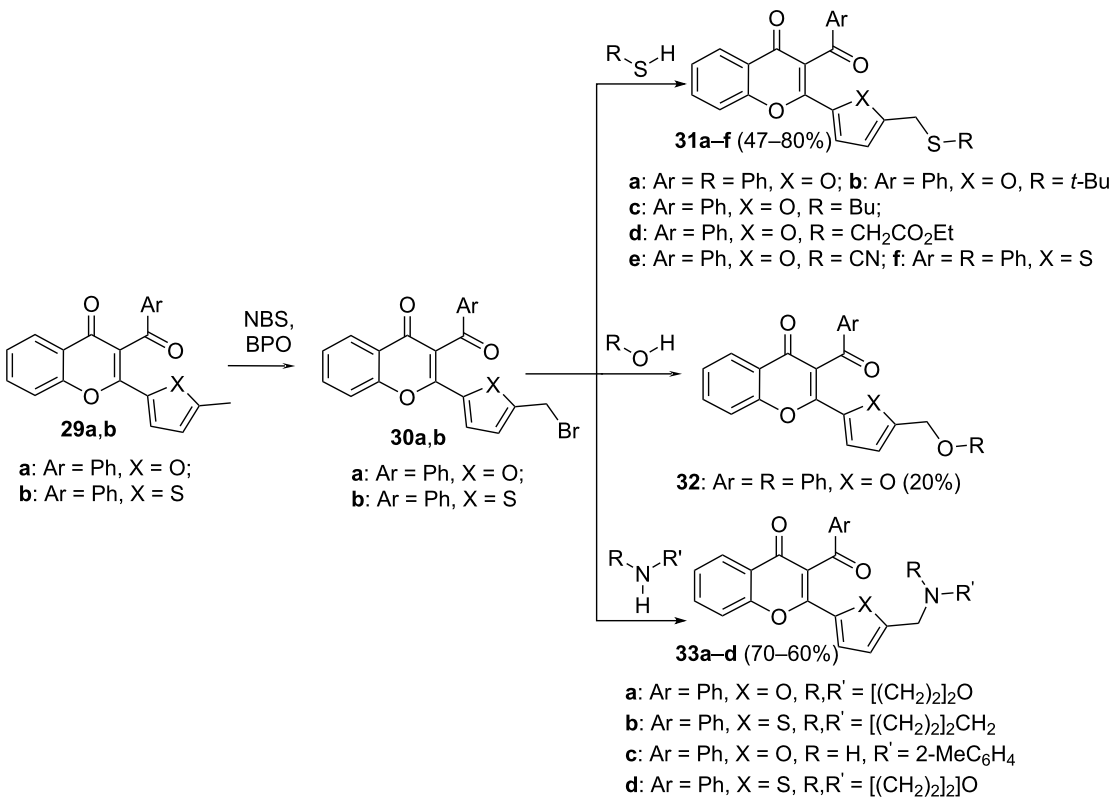
Spectral characteristics of 3-acyl-2-hetarylchromones

The spectral characteristics of 3-acyl-2-hetarylchromones – including their photosensitivity, the intensity of photoinduced fluorescence, and the ranges of absorption and fluorescence wavelengths – determine their potential as photosensitive components in data storage media. It has been demonstrated that the spectral properties of these compounds are significantly influenced by the nature of the substituents, the type of heterocyclic moiety, and the degree of conjugation within the chromone framework. Figure 2 illustrates the photoinduced changes in the absorption and fluorescence spectra of chromone **24a** in acetonitrile; these spectral shifts are representative of the behavior observed for most studied 3-acyl-2-furylchromones.

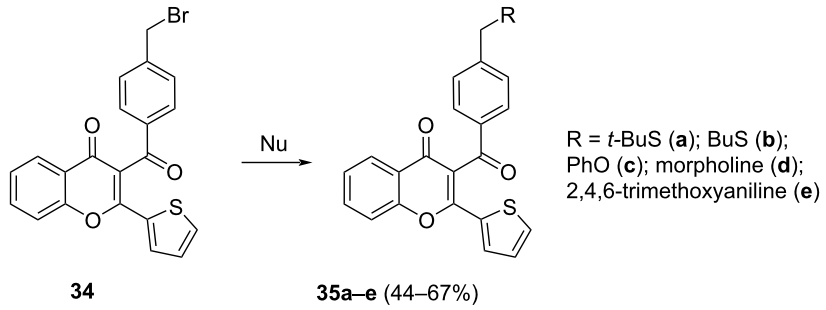
Studies of the spectral characteristics of 3-acyl-2-hetarylchromones [14,53,54,56,57] have revealed that the introduction of halogens, nitro groups, and alkyl substituents into the acyl moiety and the 6-position of the chromone induces only minor shifts in the absorption and fluorescence bands of both the parent compounds and their photoinduced forms. The photosen-



Scheme 7: Nucleophilic substitution of bromine in the furan or thiophene rings.



Scheme 8: Reactions of chromones **30a**,**b** with nucleophiles.



Scheme 9: Reactions of chromones **34** with nucleophiles.

sitivity of these compounds is predominantly governed by the nature of the substituents on the furyl substituent.

The incorporation of electron-withdrawing groups into the furan ring results in a bathochromic shift of the absorption bands for both the starting compounds and their photoproducts, whereas the positions of the fluorescence bands remain largely unchanged relative to the unsubstituted chromone. However, this modification leads to a fourfold decrease in the fluorescence quantum yield. Interestingly, the introduction of a bromine atom at the furyl moiety enhances the fluorescence intensity. Moreover, an increase in the quantum yield of the photoproduct's fluorescence is observed for compounds featuring halogens in the aroyl fragment.

3-Thienyl-2-furylchromones exhibit a substantial Stokes shift, with fluorescence intensity enhanced tenfold compared to 3-benzoyl-2-furylchromones. Replacing the furan ring with thiophene at the 2-position of the chromone markedly improves the stability of the photoinduced forms; however, these thiophene derivatives display considerably lower fluorescence intensity in the photoinduced state.

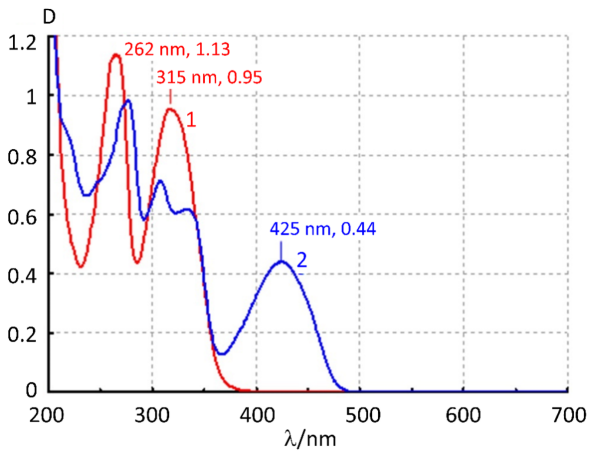


Figure 2: Absorption spectrum of chromone **24a** in acetonitrile before (1) and after (2) UV irradiation through a UFS-1 filter for 90 s.

Extending the conjugation length by incorporating benzothiophene or naphthalene units into the benzo(heteroaroyl) and furyl rings enhances the fluorescence of the photoinduced form. These compounds demonstrate a pronounced red shift in their absorption bands, while the absorption band position of the photoproduct remains essentially unaltered. The large Stokes shift is of particular practical importance for light-sensitive recording media with fluorescent readout, as it ensures a high-contrast fluorescent signal.

Mechanism of photorearrangement

The relatively low aromaticity energy of furan enables its derivatives to undergo recyclisation reactions, leading to the formation of new heterocycles. Upon irradiation, furan derivatives are promoted to the first excited triplet state, which can proceed only through cleavage of the O–Cα bond. The selectivity for a particular bond-breaking pathway is governed by a combination of energetic and kinetic factors. In the case of direct irradiation, the molecule initially reaches the singlet excited state, which can either transform into the Dewar isomer or evolve into the corresponding triplet state via intersystem crossing [58].

Experimental evidence for a triplet-state mechanism in the photorearrangement of compound **36** to **39** comes from photochemical studies that included quantum yield measurements, as well as experiments with a sensitizing agent (benzophenone) and triplet quenchers (cyclohexatriene, anthracene) [50]. The structure of photoproduct **39** was confirmed by elemental analysis and by comparison with literature analogues reported in the same study (Scheme 10) [50].

Although alternative mechanistic models have been proposed – most notably one involving carbene intermediates [53,54,59] – this pathway is not fully consistent with the available data [60,61]. For example, the carbene mechanism fails to rationalize the observation that chromone **40** (Figure 3) does not yield a fluorescent product upon UV irradiation [59].

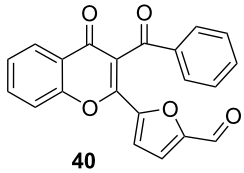
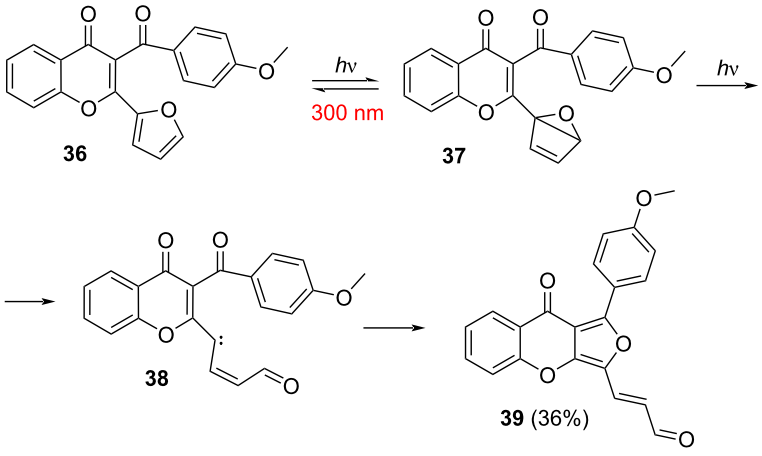


Figure 3: Chromone **40**, which does not form a fluorescent product under UV irradiation.

Ultrafast spectroscopic investigations on timescales from several hundred femtoseconds to several hundred picoseconds



Scheme 10: Photorearrangement of a 3-acyl-2-hetarylchromone **36**.

revealed the formation of a short-lived intermediate during the photorearrangement process [62]. Moreover, under multiphoton laser excitation, two distinct photoisomerization pathways were identified, each leading to a stable fluorescent photoproduct with unique spectral-luminescence characteristics [63]. Despite these advances, the precise structures of the transient intermediates and the complete mechanistic sequence remain to be fully elucidated.

Theoretical studies based on density functional theory (DFT) and time-dependent DFT (TD-DFT) provide a coherent picture of the underlying mechanism [64]. According to these calculations, UV excitation induces an electron density transfer from the furan moiety to the chromone unit. This redistribution facilitates a nucleophilic attack by the carbonyl oxygen on a carbon atom of the furan ring, followed by a rearrangement that yields furo[3,4-*b*]chromones.

Development of optical discs for archival memory

Interest in the development of optical discs continues to grow, as evidenced by market analyses such as *Global Optical Disc Market Size, Share, Growth Trends & Industry Forecast 2026–2034* [65], including ongoing research into multilayer optical storage solutions [9,66,67]. A particularly promising direction is the development of memory discs, which represent a fundamental departure from conventional CD, DVD, and Blu-ray technologies.

Unlike traditional formats, novel discs do not depend on reflective layers, which are prone to interference and transmission losses. This key distinction enables the fabrication of truly multilayer architectures capable of incorporating more than 100 information layers [68-73].

The principal advantage of this technology stems from the nonlinear mechanism of multiphoton recording, which provides markedly superior spatial localization compared to single-photon processes. In this approach, light absorption occurs exclusively within minute focal volumes or at the intersection points of two or more laser beams [69,70], where individual information voxels are encoded. Meanwhile, the surrounding material remains virtually transparent to single-photon absorption, effectively minimizing crosstalk between adjacent layers. One viable design concept for such multilayer fluorescent discs has been proposed in [74].

A diverse library of 3-acyl-2-hetarylchromones has been synthesized and successfully applied in the fabrication of photosensitive polymer films – promising candidates for archival write-once, read-many (WORM) memory systems [14-16,53,54,56,57,62,63,75]. Data recording is accomplished by exposing the medium to radiation within a defined spectral range, whereas data readout is based on detecting the luminescent signal generated upon excitation with fluorescence-inducing light. Importantly, this approach allows data to be encoded not only on the surface but also throughout the bulk of the material, enabling the construction of high-capacity multilayer optical discs [10]. This volumetric storage capability is critical for substantially increasing the information density of the storage medium.

Spin-labelled derivatives: bridging luminescence and magnetism

In recent decades, the chemistry and applications of stable organic radicals have advanced rapidly, finding relevance across numerous areas of chemistry and materials science [76]. Of particular interest are luminescent organic radicals, which have attracted considerable attention for use in organic optoelectronics [77]. The ability to understand and control spin dynamics in such luminescent radicals holds significant scientific and technological value.

It has been shown that external magnetic fields can exert a pronounced influence on the luminescence of stable organic radicals. Studies exploring the impact of magnetic fields on magneto-luminescent materials based on organic radicals provide a novel route to developing molecular photofunctionalities that can be tuned using magnetic stimuli [78]. Overcoming the theoretical and technical challenges involved in creating highly efficient luminescent organic radicals could lead to transformative developments in organic electronics [79].

Within this framework, the incorporation of stable radicals into photosensitive 3-acyl-2-hetarylchromone molecules to yield spin-labelled species with induced fluorescence represents a particularly promising strategy. This approach not only facilitates the investigation of the interplay between fluorescence and the magnetic properties of radicals but also enables the design of compounds featuring new, combined optical and magnetic functionalities.

Synthesis of hybrid spin-labelled 3-acyl-2-hetarylchromones

Two principal strategies are employed to introduce radical moieties into molecular frameworks: attaching preformed radicals to the molecular scaffold or generating radicals directly on the molecule. However, a significant challenge emerges when attaching radicals to fluorescent compounds – a commonly used approach in the preparation of spin-labelled 3-acyl-2-hetarylchromones. In many instances, this leads to either complete quenching of fluorescence [45,80] or a marked

reduction in its intensity [81,82]. This effect arises because the fluorescent center is located in the fluorophore moiety rather than in the radical itself. Fluorescence is highly sensitive to electron exchange processes between the unpaired spin of the nitroxide radical and the electrons in the conjugated system of the fluorophore [80]. Consequently, a key research question concerned whether spin-labelled 3-acyl-2-hetarylchromones – which had not been previously reported – would still yield fluorescent products upon UV-induced photorearrangement.

The present review focuses on the synthetic routes to spin-labelled 3-acyl-2-hetarylchromones and their spectral characterization. Experimental results demonstrate that UV irradiation of these spin-labelled derivatives does indeed lead to the formation of fluorescent products. This finding suggests a novel method for generating fluorescent radicals, complementing the rapidly advancing field of photogenerated luminescent radical systems [77].

It is well established that even minor chemical modifications can substantially alter the luminescent properties of radical emitters [83]. Accordingly, a series of 3-acyl-2-hetarylchromones bearing various substituents was synthesized. These compounds incorporate two types of nitroxide radicals (TEMPO and NN; see Figure 4) attached at different positions within the molecular framework.

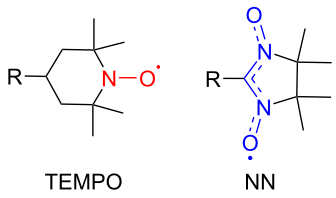
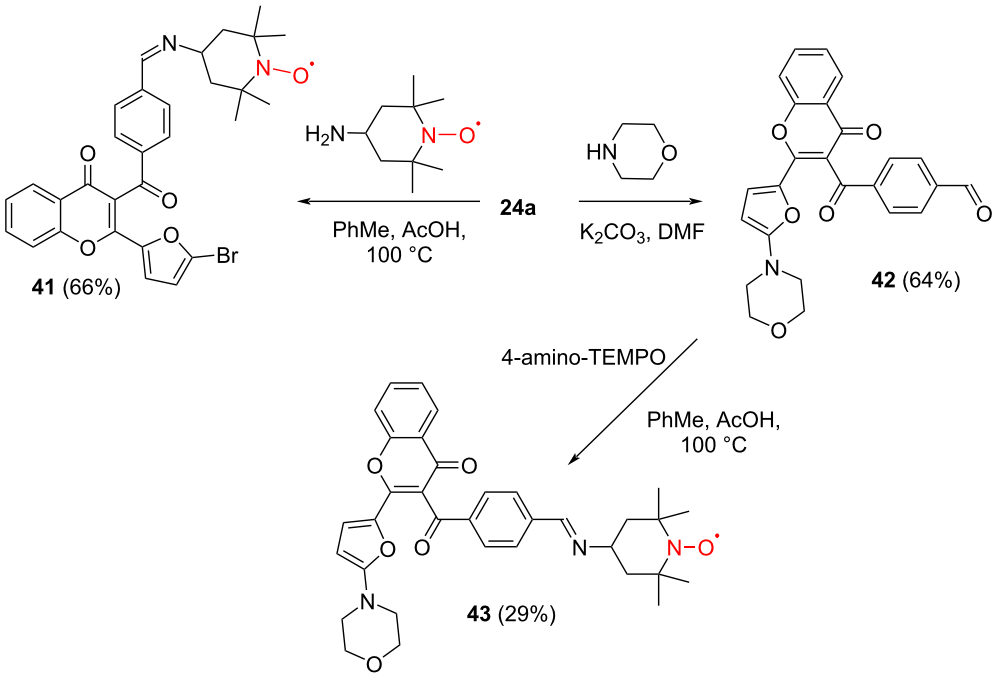


Figure 4: Nitroxide radicals (TEMPO and NN) used for spin labelling.

Synthesis of 3-acyl-2-hetarylchromones bearing a 4-amino-TEMPO moiety

4-Amino-TEMPO is a widely used building block for the construction of diverse spin-labelled compounds [84-89]. The target spin-labelled products **41** are obtained by reacting formyl chromone **24a** with 4-amino-TEMPO in toluene in the presence of acetic acid [51] (Scheme 11). A distinctive feature of derivative **41** is the spatial separation of the paramagnetic fragment from the conjugated chromone system. This structural arrangement renders it an ideal reference compound for investigating the influence of conjugation on the behavior of spin-labelled chromone derivatives.

To assess whether this trend extends to chromones bearing a piperidin-*N*-oxide substituent, spin-labelled derivative **43** was prepared by heating aldehyde **42** with 4-amino-TEMPO in toluene in the presence of a catalytic amount of acetic acid (Scheme 11) [64].



Scheme 11: Reaction of 3-acyl-2-hetarylchromones with 4-amino-TEMPO.

Single-crystal X-ray diffraction analysis of chromone **41** shows that the furan ring is nearly coplanar with the chromone core. In contrast, the benzoyl group is oriented almost orthogonally to the chromone plane, whereas the imine group lies within the plane of the aromatic ring (Figure 5) [51].

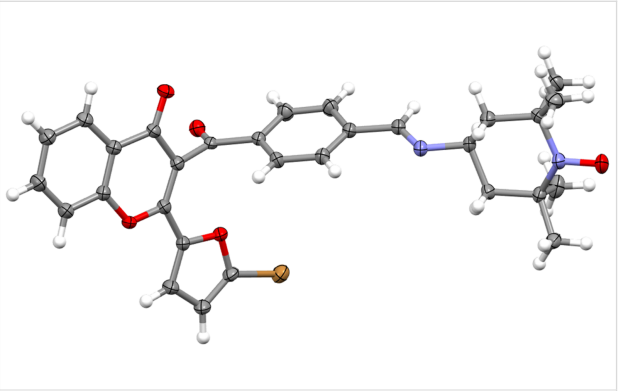


Figure 5: Molecular structure of spin-labelled chromone **41**.

Analysis of the crystal packing revealed that the nitroxide group in radical **43** forms short C–H···ONO contacts with the hydrogens of the morpholine moiety (Figure 6). Notably, the nitroxide group consistently exhibits a preference for forming these short contacts with the morpholine hydrogens rather than with the methyl hydrogens from the CMe_2–NO fragments [64].

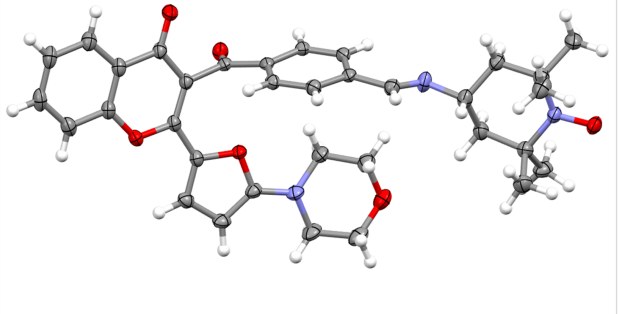


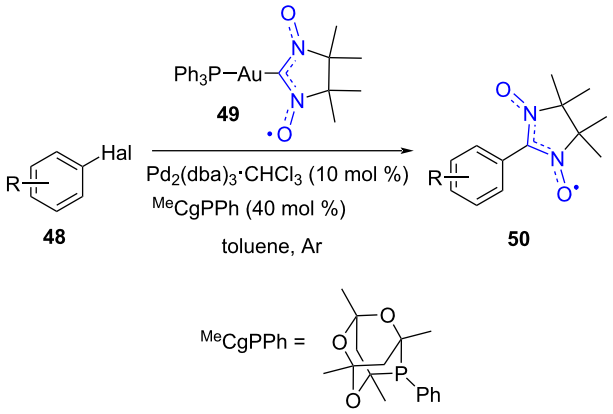
Figure 6: Molecular structure of nitroxide **43**.

Synthesis of 3-acyl-2-hetarylchromones containing nitronyl nitroxides

The development of spin-labelled 3-acyl-2-hetarylchromone derivatives bearing nitronyl nitroxide moieties relies on two principal synthetic strategies:

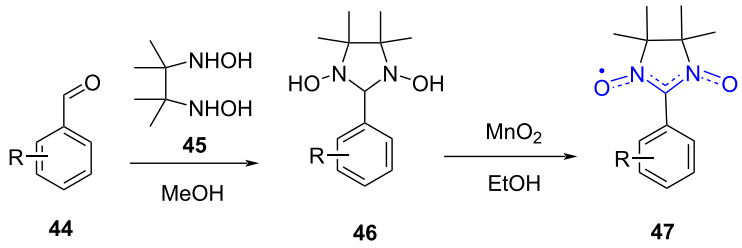
1. The oxidation of adducts formed between formyl chromone derivatives and 2,3-bis(hydroxylamino)-2,3-dimethylbutane [90] (Scheme 12).

2. Palladium-catalyzed cross-coupling of organometallic nitronyl nitroxide derivatives with aryl halides (Scheme 13) [91,92].

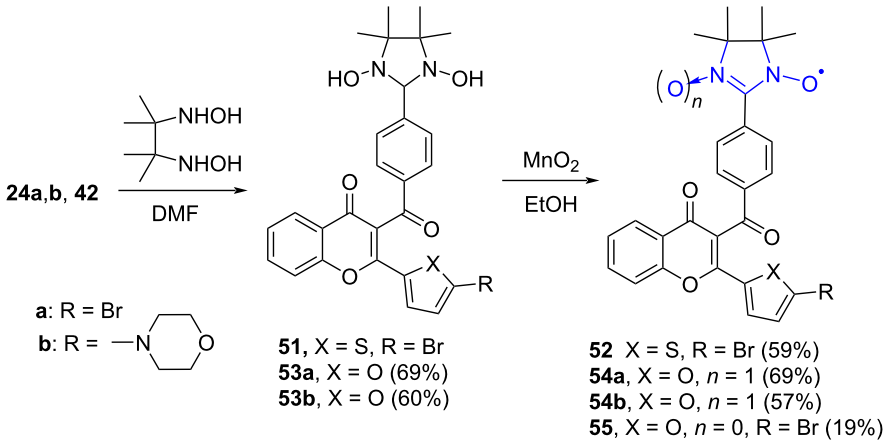


Scheme 13: Preparation of nitronyl nitroxides through cross-coupling reactions.

The first synthetic strategy involves the condensation of formyl chromone **24b** with vicinal bis-hydroxylamine in DMF under an argon atmosphere at room temperature, affording **51** as the 1,3-dihydroxyimidazolidine intermediate. Oxidation to the corresponding spin-labelled chromone **52** was carried out in ethanol at ambient temperature using an excess of manganese dioxide (Scheme 14) [52].



Scheme 12: Synthesis of nitronyl nitroxides via condensation of aldehydes with 2,3-bis(hydroxylamino)-2,3-dimethylbutane.



Scheme 14: Synthesis of nitronyl nitroxides **52**, **54a**, **54b**, and iminonitroxide **55**.

Analogously, aldehydes **24a** and **42** were subjected to condensation with vicinal bishydroxylamine in DMF to yield the respective 1,3-dihydroxyimidazolidines **53a**,**b**. Subsequent oxidation under mild conditions with manganese dioxide afforded the target nitronyl nitroxides **54a**,**b**. During the synthesis of nitronyl nitroxide **54a**, a side product – the iminonitroxide analogue **55** – was isolated in a low yield of 19% (Scheme 14) [64]. This by-product formation is consistent with the redox lability of nitronyl nitroxide precursors under oxidative conditions.

All nitroxides were comprehensively characterized both in solution and in the solid state [64]. In compounds **54a** and **54b**, the furan rings are nearly coplanar with the adjacent chromone core. Meanwhile, the carbonyl groups adopt orientations close to the planes of the phenyl fragments and are markedly twisted relative to the chromone framework (Figure 7).

Chromone **58**, featuring a nitronyl nitroxide functionality, was synthesized by means of a Pd-catalyzed cross-coupling reaction between halo-substituted chromone precursors **25a**, **56** and an organogold derivative of 4,4,5,5-tetramethyl-2-imidazoline-3-oxide-1-oxide **57** (Scheme 15) [93]. Among the tested precursors, the bromo-derivative **25a** proved especially effective, enabling isolation of the target nitronyl nitroxide product in yields of up to 70%. In contrast, the iodo-analogue **56** provided the corresponding product in a lower yield of 47%.

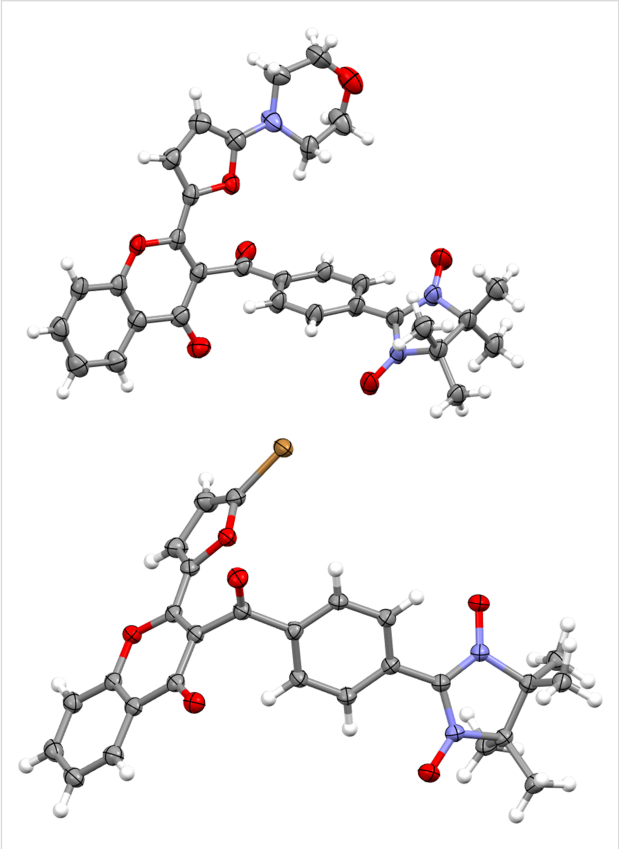
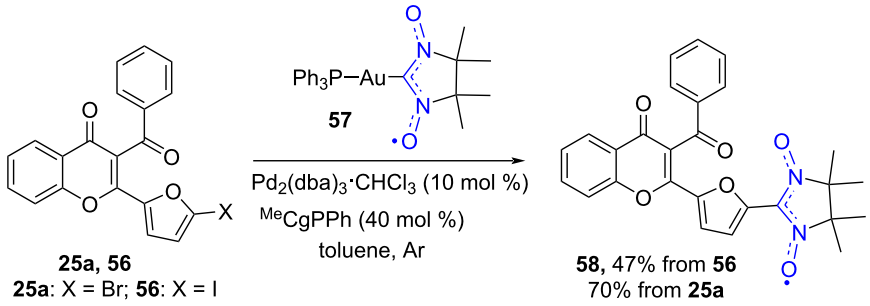


Figure 7: Molecular structures of nitronyl nitroxides **54a** (up) and **54b** (down).

Single-crystal X-ray diffraction analysis of compound **58** revealed the presence of two crystallographically independent molecules in the unit cell (Figure 8). The imidazolidine ring adopts a twisted conformation, with the two carbon atoms of the CMe_2 moieties displaced from the plane defined by the remaining three ring atoms. The planes of the furan rings are rotated relative to those of the adjacent paramagnetic fragments by angles of 20.5° and 21.3°; at the same time, the furan rings are nearly coplanar with the neighboring pyranone moieties. The carbonyl groups lie almost in the plane of the phenyl fragments and are markedly rotated relative to the plane of the chromone backbone, with corresponding dihedral angles of 75.0° and 76.3°.



Scheme 15: Synthesis of a chromone containing nitronyl nitroxide group.

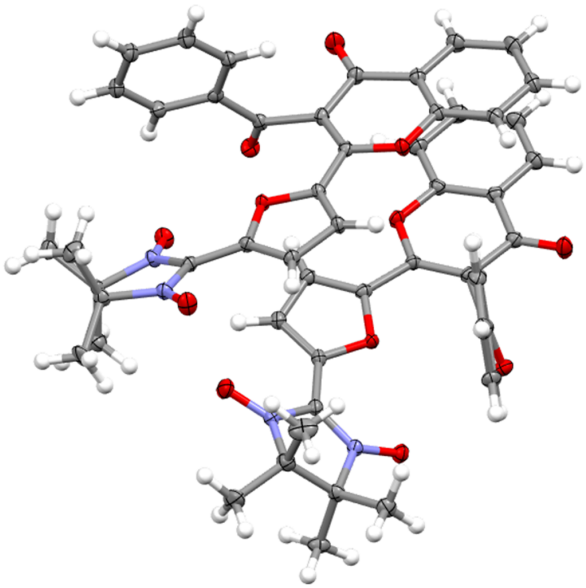


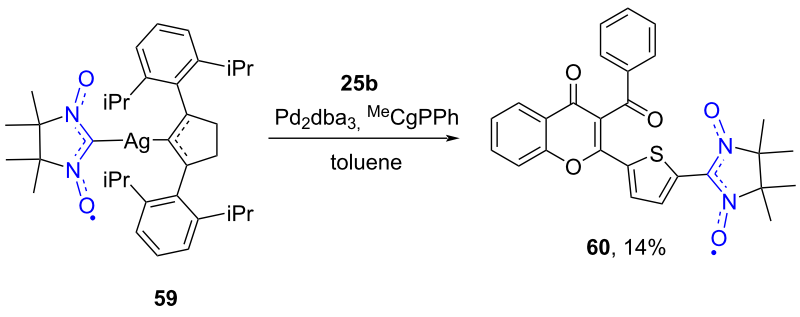
Figure 8: Structure of two crystallographically independent molecules of **58**. Thermal ellipsoids for non-hydrogen atoms are shown at the 50 % probability level.

A particularly notable feature of the crystal structure of **58** is the existence of short intermolecular contacts (3.090 Å) between the O and C atoms of the nitronyl nitroxide fragments. This distance is shorter than the sum of the van der Waals radii of carbon and oxygen (3.35 Å). The O atom carries a negative spin density, whereas the C atom bears a positive spin density. According to the McConnell model [94], such short contacts can act as pathways for relatively strong ferromagnetic exchange interactions [95,96].

The cross-coupling reaction between an organosilver derivative of 4,4,5,5-tetramethyl-2-imidazoline-3-oxide-1-oxide **59** and the bromo-substituted thiophene-containing chromone **25b** afforded 3-acyl-2-thienylchromone **60**, which bears a conjugated radical (Scheme 16) [52].

According to X-ray diffraction data, the molecular structure of compound **60** differs from that of its furan-substituted analogue (Figure 9). The plane of the thiophene ring is rotated relative to that of the adjacent paramagnetic fragment by an angle of 6.1°; while the angle between the thiophene ring and the neighbouring pyranone moiety equals 18.8°. The carbonyl group lies almost in the plane of the phenyl fragment and is significantly rotated relative to the plane of the chromone backbone, with a corresponding dihedral angle of 87.8°.

The successful crystallization and structural characterization of nitronyl nitroxide **60** allowed us to confirm its molecular architecture; however, its pronounced instability in both solution and solid states remains a critical limitation. Multiple decomposi-



Scheme 16: Synthesis of 3-acyl-2-thienylchromone **60** containing a conjugated nitronyl nitroxide radical.

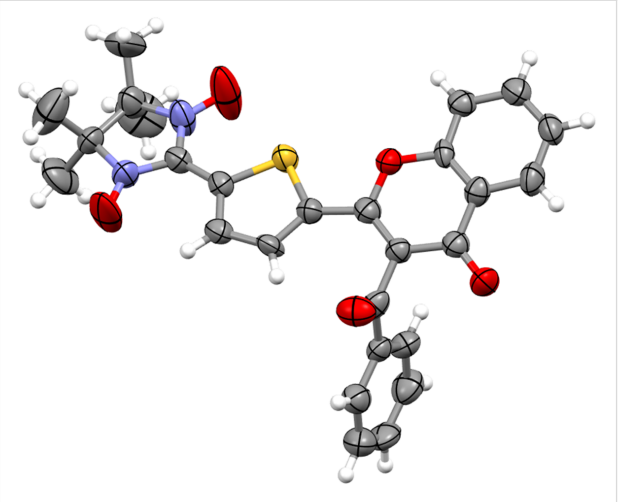


Figure 9: Structure of 3-acyl-2-thienylchromone **60**. Thermal ellipsoids for non-hydrogen atoms are shown at the 50% probability level.

tion pathways were observed, with formation of the corresponding iminonitroxide as one of the detectable products. A particularly informative comparison is with analogue **58**, bearing a furyl substituent: under identical conditions, **58** demonstrates markedly higher stability, indicating a strong influence of the heteroaryl moiety and its substitution position on the radical's robustness. This observation aligns with our earlier findings on α-substituted thiophene derivatives, where nitronyl nitroxide moieties exhibited good stability [97], further supporting the notion that the lability of **60** stems from its specific electronic and steric profile rather than from the presence of a thiophene ring.

Comparison of spectral characteristics of spin-labelled 3-acyl-2-hetarylchromones, their photochemical behavior and structure–property relationships

The electronic absorption spectra of 3-acyl-2-hetarylchromones are fairly consistent across the series of compounds that differ in the substituents on the acyl moiety of the chromone molecule. The impact of these substituents on the electronic spectrum of the chromone skeleton is relatively minor. This can be attributed to the fact that, according to X-ray diffraction data, the acyl group is oriented nearly perpendicular to the plane of the chromone skeleton and is therefore largely excluded from conjugation with it. For example, the spectra of the bromo-derivatives – 3-benzoyl-2-(5-bromofuryl)-4*H*-chromen-4-ones (compounds **24a**, **25a**, and **53a**) – display highly intense absorption bands in the 240–280 nm region, as well as very intense bands in the 310–350 nm range (Figure 10, Table 1). The latter bands correspond to a combination of electronic transitions from the HOMO to the LUMO, as confirmed by TD-DFT analysis [64]. In contrast, for compounds **28**, **42**, and **53b**, which feature a morpholine substituent in the five-membered heterocycle, the short-wavelength intense band remains in the same region, whereas the long-wavelength band undergoes a pronounced bathochromic shift, moving to the 400–430 nm range (Figure 11).

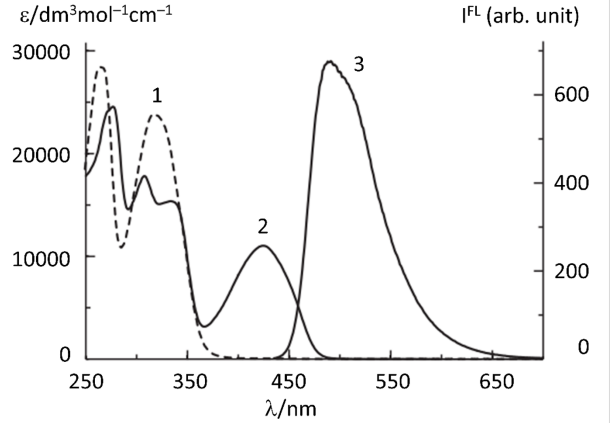


Figure 10: Absorption spectra of compound **24a** in acetonitrile before (curve 1) and after (2) UV irradiation through an UFS-1 optical filter (240–420 nm) for 1.5 min upon reaching the maximum luminescence intensity; the luminescence spectrum (curve 3) recorded upon excitation at a wavelength of 425 nm. Figure 10 was reproduced from [51], *Mendeleev Commun.*, vol. 34, by K. V. Agliulin, A. V. Stepanov, V. N. Yarovenko, M. M. Krayushkin, E. V. Tretyakov, D. I. Nasyrova, V. V. Ilyushenkova, A. O. Ayt, T. M. Valova,, "Synthesis, structure and properties of spin-labeled photosensitive chromone derivative", p. 828-830, Copyright (2024) with permission from *Mendeleev Communications*. Published by Elsevier on behalf of the N. D. Zelinsky Institute of Organic Chemistry of the Russian Academy of Sciences. This content is not subject to CC BY 4.0.

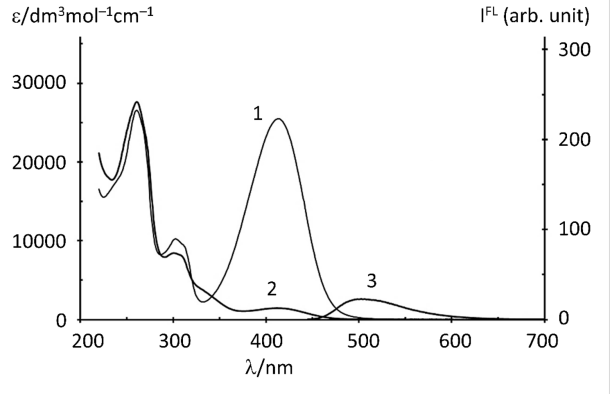


Figure 11: Absorption spectra of compound **42** in acetonitrile before (curve 1) and after (2) UV irradiation through an SZS-21 optical filter (350–560 nm) for 30 min upon reaching the maximum luminescence intensity; the luminescence spectrum (curve 3) recorded upon excitation at a wavelength of 445 nm. Figure 11 was reproduced from [64], K. V. Agliulin et al., "Chromones Functionalized with Nitroxide Radicals: Synthesis, Structural Characterization, and Photoinduced Luminescence Switching", *Asian J. Org. Chem.*, with permission from John Wiley and Sons. Copyright © 2026 Wiley-VCH GmbH. This content is not subject to CC BY 4.0.

A characteristic feature of the studied 3-acyl-2-hetaryl-chromones is their lack of intrinsic luminescence before irradiation. Upon exposure to UV light in acetonitrile ($c \approx 4 \times 10^{-5}$ M), a new luminescence band appears in the 490–520 nm range, concomitant with changes in the absorption spectrum (Figure 10 and Figure 11). Notably, the luminescence intensity displayed a non-monotonic profile during irradiation: it initially increased and subsequently decreased. This behavior indicates the occurrence of secondary photochemical processes in addition to the primary photoisomerization of the chromone scaf-

Table 1: Spectral and fluorescence characteristics of 3-aroyl-2-(2-furyl)chromones before and after UV irradiation.

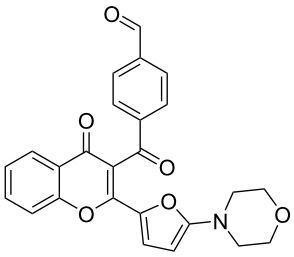
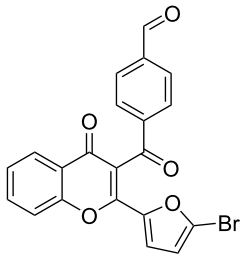
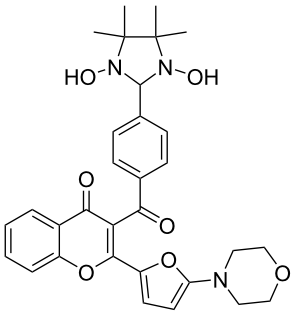
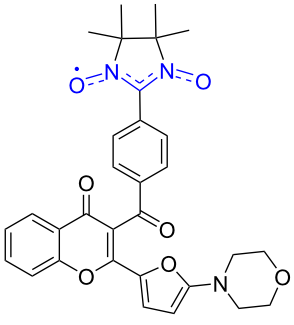
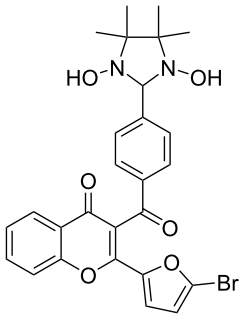
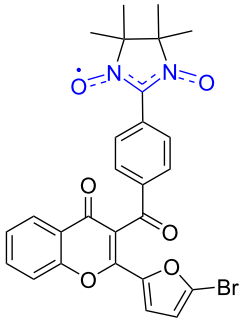
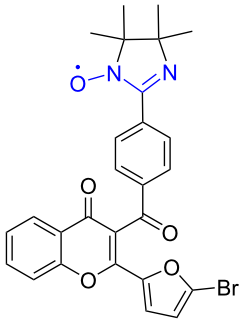
Compound	Absorption spectra, λ_{max}, nm (ε, $dm^3mol^{-1}cm^{-1}$)		Fluorescence spectra, λ_{max}, nm (*I*, arb. unit)
	Initial form	After irradiation	After irradiation
 **42**	278 (32200), 417 (25430)	278 (32200), 435 (4140)	510 (60)
 **24a**	261 (26540), 303 (10240), 414 (25480)	261 (27610), 301 (8450), 411 (1450)	503 (23)
 **53b**	252 (20360), 302 (8540), 313 (7570), 413 (22720)	259 (24780), 307 (13090), 334 (11240), 420 (6580)	514 (123)
 **54b**	241 (23220), 307 (24000), 396 (26800)	247 (23950), 306 (13240), 388 (3620)	503 (45)

Table 1: Spectral and fluorescence characteristics of 3-aroyl-2-(2-furyl)chromones before and after UV irradiation. (continued)

 **53a**	268 (21600), 323 (26600)	268 (21600), 312 (23800), 396 (5300), 430 (4200)	491 (230)
 **54a**	246 (20500), 273 (16000), 315 (42500), 395 (7500)	246 (22700), 272 (20400), 314 (25500), 394 (6500), 430 (4800)	494 (290)
 **55**	271 (16600), 317 (15500), 323 (15400)	270 (13300), 309 (11000), 330 (9500), 427 (4400)	494 (250)

fold. To date, the detailed nature of these secondary transformations remains unreported in the literature. The extent of these processes is influenced by the substitution pattern in the chromone core. For the bromo derivative **24a**, the maximum luminescence intensity, as indicated by the electronic spectra, is reached at incomplete conversion. In contrast, for the initial aldehyde **42** bearing a morpholine substituent, the intense absorption band in the 395–415 nm region nearly disappears from its electronic spectrum upon irradiation. This disappearance indicates a high degree of conversion of the parent 3-aroyl-2-(2-furyl)chromones into corresponding furo[3,4-*b*]chromone-3-acrolein derivatives [64].

The introduction of a paramagnetic substituent served three purposes. First, it was necessary to determine whether a chromone bearing a paramagnetic group is capable of undergoing photoisomerization. Second, it was important to establish whether the nature and position of the paramagnetic group influence both the photoisomerization process and the subsequent formation of luminescent products. Third, if photoisomerization is feasible, it was essential to ascertain whether degradation of the radical group and the emergence of luminescence would be observed.

Notably, spin-labelled 3-acyl-2-hetarylchromones bearing paramagnetic substituents in the acyl moiety exhibit the same most intense absorption bands in their electronic spectra as their diamagnetic precursors. In addition, all radicals display weak long-wavelength bands in the visible region. These bands correspond to a superposition of two transitions: an α-electron

promotion from the SOMO to the LUMO and a β-electron transition from the HOMO to the counterpart of the SUMO [64].

All spin-labelled 3-acyl-2-hetarylchromones do not exhibit any luminescence prior to irradiation. UV irradiation of the TEMPO-substituted chromones **41** and **43** was shown to induce their transformation into products characterized by an absorption band in the visible region with a maximum at 425 nm and an intense luminescence band with a maximum at 510 nm (Figure 12 and Figure 13).

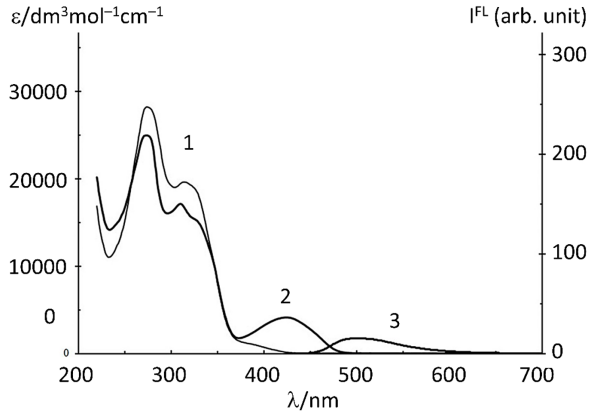


Figure 12: Absorption spectra of compound **41** in acetonitrile before (curve 1) and after (2) UV irradiation through an UFS-1 optical filter (240–420 nm) for 5 min upon reaching the maximum luminescence intensity (3); the luminescence spectrum was recorded upon excitation at 423 nm. Figure 12 was reproduced from [51], *Mendeleev Commun*., vol. 34, by K. V. Agliulin, A. V. Stepanov, V. N. Yarovenko, M. M. Krayushkin, E. V. Tretyakov, D. I. Nasyrova, V. V. Ilyushenkova, A. O. Ayt, T. M. Valova, "Synthesis, structure and properties of spin-labeled photosensitive chromone derivative", p. 828–830, Copyright (2024) with permission from *Mendeleev Communications*. Published by Elsevier on behalf of the N. D. Zelinsky Institute of Organic Chemistry of the Russian Academy of Sciences. This content is not subject to CC BY 4.0.

Importantly, the TEMPO moiety demonstrated remarkable photostability under irradiation at 312 nm. This was confirmed by the absence of changes in the EPR signal intensity for the irradiated solution, indicating that the nitroxide radical center remained intact. The observed stability can be attributed to the significantly faster rate of chromone photoisomerization relative to any photoinduced transformation of the TEMPO unit.

Upon UV irradiation of acetonitrile solutions of nitroxide-substituted chromones **41** and **43**, the maximum luminescence intensity at 510 nm was reached within 3–5 min. In contrast, the phototransformation of free TEMPO in acetonitrile requires prolonged irradiation (tens of hours) using PRP 3000 lamps [98]. This process involves initial hydrogen abstraction by the excited nitroxide from MeCN, followed by recombination of the resulting $^{\bullet}CH_2CN$ radical with TEMPO. The stark difference in time scales underscores the kinetic dominance of the chromone photoreaction over the side photochemistry of the TEMPO label.

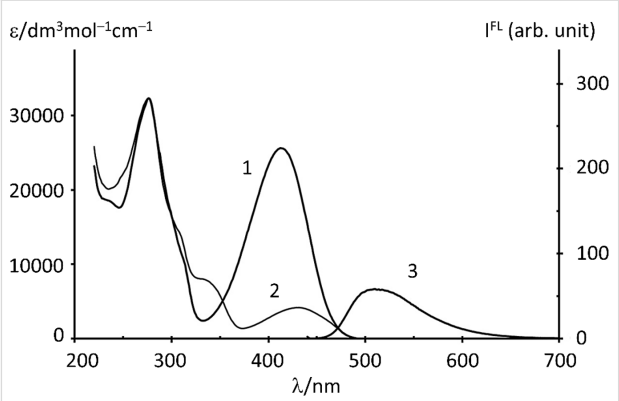


Figure 13: Absorption spectra of compound **43** in acetonitrile before (curve 1) and after (2) UV irradiation through an UFS-5 optical filter (250–400 nm) for 3 min upon reaching the maximum luminescence intensity (3); the luminescence spectrum was recorded upon excitation at 423 nm. Figure 13 was reproduced from [64], K. V. Agliulin et al., "Chromones Functionalized with Nitroxide Radicals: Synthesis, Structural Characterization, and Photoinduced Luminescence Switching", *Asian J. Org. Chem.*, with permission from John Wiley and Sons. Copyright © 2026 Wiley-VCH GmbH. This content is not subject to CC BY 4.0.

The photochemical behavior of chromones **54a**, **54b**, and **55** was investigated by UV irradiation through an UFS-5 filter (250–400 nm). The observed partial to complete loss of the absorption band at 395–415 nm confirms the transformation of the parent 3-aroyl-2-(2-furyl)chromones into furo[3,4-*b*]chromone-3-acrolein derivatives. However, the absence of isosbestic points in the UV–vis spectra (e.g., for **54a**) implies that the phototransformation involves more than two absorbing species, ruling out a simple 1:1 stoichiometric pathway (Figure 14).

EPR monitoring provides further insight into the mechanism. Complete disappearance of the paramagnetic signal upon irradiation at 312 nm for 1 h indicates full consumption of the radical moiety under these conditions. In contrast, the partial attenuation of the EPR signal at 400 nm suggests incomplete conversion. This wavelength-dependent behavior implies that efficient hydrogen abstraction requires the nitronyl nitroxide group to access an upper excited state, which is more readily populated at shorter wavelengths.

Similarly, upon irradiating with light from a xenon lamp through a UFS-1 or UFS-5 filter, the thienyl-substituted derivative **52** undergoes transformation. This is evidenced by changes in the electronic absorption spectra and the emergence of a luminescence band with a peak in the 491–514 nm range. The ir-

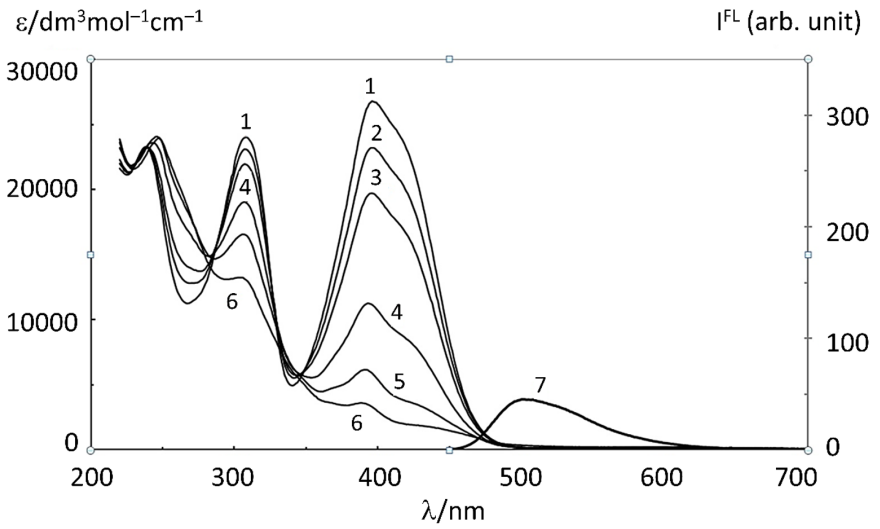


Figure 14: Changes in the initial absorption spectrum (curve 1) of compound **54a** upon UV irradiation through an UFS-5 optical filter (250–400 nm) for 3, 5, 10, 15, and 30 min (curves 2–6, respectively); the luminescence spectrum (curve 7) recorded upon excitation at a wavelength of 445 nm for 30 min. Figure 14 was reproduced from [64], K. V. Agliulin et al., "Chromones Functionalized with Nitroxide Radicals: Synthesis, Structural Characterization, and Photoinduced Luminescence Switching", *Asian J. Org. Chem.*, with permission from John Wiley and Sons. Copyright © 2026 Wiley-VCH GmbH. This content is not subject to CC BY 4.0.

radiation was carried out for 5 minutes, which corresponded to the time required to achieve the maximum increase in luminescence intensity. Notably, during the irradiation of radical **52**, the intense absorption band at 315 nm nearly disappears from its electronic spectrum (Figure 15). This disappearance indicates a high degree of conversion of the radical into a luminescent product.

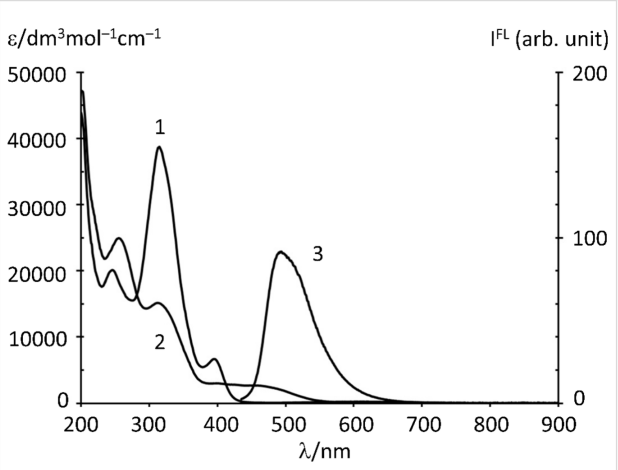


Figure 15: Absorption spectra of compound **52** in acetonitrile: (1) before irradiation; (2) after 5 min of UV irradiation through a UFS-1 or UFS-5 filter; (3) luminescence spectrum recorded upon reaching the maximum luminescence intensity.

In contrast to the spin-labelled chromones discussed above, the paramagnetic derivatives **58** and **60** – featuring a nitronyl nitroxide group directly attached to the furan or thiophene ring – do not undergo photorearrangement. This is evidenced by the fact that their absorption spectrum remains virtually unchanged after 5 minutes of UV irradiation through a UFS-1 filter. These results indicate that the photorearrangement process is suppressed when paramagnetic substituents are located directly on the heterocyclic ring. In contrast, substituents positioned in the acyl moiety of the molecule do not inhibit the transformation. This structural sensitivity underscores the critical role of the radical's placement in modulating the photochemical reactivity of these hybrid systems.

Conclusion

This review highlights the unique photochemical behavior of 3-acyl-2-hetarylchromones containing (*Z*)-3-(2-furyl)- or (*Z*)-3-(2-thienyl)-1-arylpropenone moieties [F(T)AP]. Upon UV irradiation, these compounds undergo an irreversible rearrangement to yield fluorescent species. This transformation holds substantial value both for fundamental research into photochemical mechanisms and for practical implementation, including the design of multilayer storage media for archival optical memory.

The available synthetic methodologies for introducing diverse substituents into the chromone scaffold demonstrate the flexibility and broad applicability of the current approaches. In light of the rapid advances in the chemistry of stable radicals and photoactive compounds, the development of spin-labelled photoactive chromones represents a highly promising research

direction. These hybrid systems combine photoactivity with magnetic functionality, enabling the creation of multifunctional molecular devices.

A particularly important finding is the first demonstration that a stable radical can either amplify or diminish the intensity of induced fluorescence, with the outcome dictated by the specific substituents on the chromone core. This tunable interplay between fluorescence and radical moieties opens new avenues for engineering molecular switches with light-responsive characteristics. To fully capture the interplay between optical and magnetic properties, integrated experimental workflows combining photophysical measurements (steady-state and time-resolved spectroscopy) with magnetic characterization (EPR, SQUID) are required.

Overall, spin-labelled 3-acyl-2-hetarylchromones offer a powerful platform for exploring the synergy between fluorescence and magnetic properties. The resulting insights not only deepen the fundamental understanding of excited-state spin phenomena but also pave the way for multifunctional materials with applications ranging from advanced data storage to stimuli-responsive functional systems.

Author Contributions

Mikhail M. Krayushkin: writing – review & editing. Evgeny V. Tretyakov: writing – review & editing. Vladimir N. Yarovenko: conceptualization.

ORCID® iDs

Mikhail M. Krayushkin - https://orcid.org/0000-0002-2719-2861
Evgeny V. Tretyakov - https://orcid.org/0000-0003-1540-7033
Vladimir N. Yarovenko - https://orcid.org/0000-0003-3153-6791

Data Availability Statement

Data sharing is not applicable as no new data was generated or analyzed in this study.

References

1. Gaspar, A.; Garrido, E. M. P. J.; Borges, F.; Garrido, J. M. P. J. *ACS Omega* **2024,** *9,* 21706–21726. doi:10.1021/acsomega.4c00771
2. Abo-Salem, H. M.; El Souda, S. S. M.; Shafey, H. I.; Zoheir, K. M. A.; Ahmed, K. M.; Mahmoud, K.; Mahrous, K. F.; Fawzy, N. M. *Sci. Rep.* **2024,** *14,* 9636. doi:10.1038/s41598-024-59606-2
3. Shakibay Senobari, Z.; Masoumian Hosseini, M.; Teimouri, M. B.; Rezayan, A. H.; Samarghandian, S.; Hekmat, A. *BMC Res. Notes* **2023,** *16,* 224. doi:10.1186/s13104-023-06508-7
4. Sharma, K. *ChemistrySelect* **2022,** *7,* e202200540. doi:10.1002/slct.202200540
5. Mohsin, N. u. A.; Irfan, M.; Hassan, S. u.; Saleem, U. *Pharm. Chem. J.* **2020,** *54,* 241–257. doi:10.1007/s11094-020-02187-x
6. Kladova, O. A.; Kuznetsova, A. A.; Barthes, N. P. F.; Michel, B. Y.; Burger, A.; Fedorova, O. S.; Kuznetsov, N. A. *Russ. J. Bioorg. Chem.* **2019,** *45,* 599–607. doi:10.1134/s1068162019060220
7. Huang, P.; Lu, J.; Jin, L.; Liu, E.; Li, L. *J. Fluoresc.* **2023,** *33,* 453–458. doi:10.1007/s10895-022-03095-x
8. Hermanto, N. A.; Juahir, Y.; Mustafar, S.; Sharif, A. M.; Osman, U. M.; Ulianas, A. *J. Sci. Math. Lett.* **2024,** *12,* 161–169. doi:10.37134/jsml.vol12.2.13.2024
9. Yan, Z.; Hu, J.; Xiao, Z.; Xie, D.; Cao, Q.; Gan, Z.; Zhang, J. *Chin. Opt. Lett.* **2023,** *21,* 120051. doi:10.3788/col202321.120051
10. Barachevsky, V.; Krayushkin, M.; Kiyko, V. Light-Sensitive Organic Recording Media for Three-Dimensional Optical Memory. In *Photon-Working Switches;* Yokoyama, Y.; Nakatani, K., Eds.; Springer: Tokyo, 2017; pp 181–207. doi:10.1007/978-4-431-56544-4_9
11. Migulin, V. A.; Lvov, A. G.; Krayushkin, M. M. *Tetrahedron* **2017,** *73,* 4439–4449. doi:10.1016/j.tet.2017.06.005
12. Chudov, K. A.; Levchenko, K. S.; Yarovenko, V. N.; Krayushkin, M. M.; Barachevsky, V. A.; Baryshnikova, T. K.; Grebennikov, E. P. *Russ. Chem. Bull.* **2015,** *64,* 405–409. doi:10.1007/s11172-015-0876-8
13. Chudov, K. A.; Levchenko, K. S.; Barachevskii, V. A.; Valova, T. M.; Grebennikov, E. P.; Shmelin, P. S.; Poroshin, N. O.; Adamov, G. E.; Yarovenko, V. N.; Krayushkin, M. M. *Mendeleev Commun.* **2016,** *26,* 521–523. doi:10.1016/j.mencom.2016.11.021
14. Krayushkin, M. M.; Levchenko, K. S.; Yarovenko, V. N.; Zavarzin, I. V.; Barachevsky, V. A.; Puankov, Y. A.; Valova, T. M.; Kobeleva, O. I. *ARKIVOC* **2009,** No. ix, 269–283. doi:10.3998/ark.5550190.0010.916
15. Martynov, I. Y.; Barachevsky, V. A.; Ayt, A. O.; Kobeleva, O. I.; Valova, T. M.; Levchenko, K. S.; Yarovenko, V. N.; Krayushkin, M. M. *Opt. Mater. (Amsterdam, Neth.)* **2014,** *37,* 488–492. doi:10.1016/j.optmat.2014.07.011
16. Krajushkin, M. M.; Jarovenko, V. N.; Levchenko, K. S.; Zavarzin, I. V.; Barachevskij, V. A.; P'jankov, J. A.; Kobeleva, O. I.; Valova, T. M.; Mikhal, I. Irreversible photosensitive organic systems based on chromone derivatives for photonics. RU Patent 2,374,237 C1, Nov 27, 2009, https://patents.google.com/patent/RU2374237C1/en.
17. Tretyakov, E. V.; Ovcharenko, V. I.; Terent'ev, A. O.; Krylov, I. B.; Magdesieva, T. V.; Mazhukin, D. G.; Gritsan, N. P. *Russ. Chem. Rev.* **2022,** *91,* RCR5025. doi:10.1070/rcr5025
18. Tretyakov, E. V. Preparation and characterization of magnetic and magnetophotonic materials based on organic free radicals. In *Organic Radicals;* Wang, C.; Labidi, A.; Lichtfouse, E., Eds.; Elsevier, 2024; pp 61–181. doi:10.1016/b978-0-443-13346-6.00005-1
19. Kubo, T.; Abe, M. *Chem. Rev.* **2024,** *124,* 4541–4542. doi:10.1021/acs.chemrev.3c00893
20. Zhang, Y.; Qiu, R.; Qu, K.; Zhang, C.; Stoddart, J. F.; Chen, H. *Sci. China Mater.* **2024,** *67,* 709–728. doi:10.1007/s40843-024-2792-0
21. Nguyen, H. V.-T.; Chen, Q.; Paletta, J. T.; Harvey, P.; Jiang, Y.; Zhang, H.; Boska, M. D.; Ottaviani, M. F.; Jasanoff, A.; Rajca, A.; Johnson, J. A. *ACS Cent. Sci.* **2017,** *3,* 800–811. doi:10.1021/acscentsci.7b00253
22. Khramtsov, V. V. *Antioxid. Redox Signaling* **2018,** *28,* 1365–1377. doi:10.1089/ars.2017.7329
23. Ji, L.; Shi, J.; Wei, J.; Yu, T.; Huang, W. *Adv. Mater. (Weinheim, Ger.)* **2020,** *32,* 1908015. doi:10.1002/adma.201908015
24. Asanbaeva, N. B.; Dobrynin, S. A.; Morozov, D. A.; Haro-Mares, N.; Gutmann, T.; Buntkowsky, G.; Bagryanskaya, E. G. *Molecules* **2023,** *28,* 1926. doi:10.3390/molecules28041926
25. Hou, X.; Xu, T.; Zhu, J.; Wu, S.; Wu, J. *Chemistry* **2025,** *7,* 21. doi:10.3390/chemistry7010021

26. Janoschka, T.; Hager, M. D.; Schubert, U. S. *Adv. Mater. (Weinheim, Ger.)* **2012,** *24,* 6397–6409. doi:10.1002/adma.201203119
27. Suga, T.; Ohshiro, H.; Sugita, S.; Oyaizu, K.; Nishide, H. *Adv. Mater. (Weinheim, Ger.)* **2009,** *21,* 1627–1630. doi:10.1002/adma.200803073
28. Gaudenzi, R.; Burzurí, E.; Reta, D.; Moreira, I. de P. R.; Bromley, S. T.; Rovira, C.; Veciana, J.; van der Zant, H. S. J. *Nano Lett.* **2016,** *16,* 2066–2071. doi:10.1021/acs.nanolett.6b00102
29. Frisenda, R.; Gaudenzi, R.; Franco, C.; Mas-Torrent, M.; Rovira, C.; Veciana, J.; Alcon, I.; Bromley, S. T.; Burzurí, E.; van der Zant, H. S. J. *Nano Lett.* **2015,** *15,* 3109–3114. doi:10.1021/acs.nanolett.5b00155
30. Slota, M.; Keerthi, A.; Myers, W. K.; Tretyakov, E.; Baumgarten, M.; Ardavan, A.; Sadeghi, H.; Lambert, C. J.; Narita, A.; Müllen, K.; Bogani, L. *Nature* **2018,** *557,* 691–695. doi:10.1038/s41586-018-0154-7
31. Zhou, A.; Sun, Z.; Sun, L. *Innovation* **2024,** *5,* 100662. doi:10.1016/j.xinn.2024.100662
32. Kolesnikov, A. E.; Bryzgalov, A. O.; Tolstikov, S. E.; Yanshole, V. V.; Romanenko, G. V.; Letyagin, G. A.; Smirnova, K. A.; Tolstikova, T. G.; Bogomyakov, A. S.; Ovcharenko, V. I. *Nitric Oxide* **2024,** *143,* 9–15. doi:10.1016/j.niox.2023.12.001
33. Bagryanskaya, E. G.; Krumkacheva, O. A.; Fedin, M. V.; Marque, S. R. A. *Methods Enzymol.* **2015,** *563,* 365–396. doi:10.1016/bs.mie.2015.06.004
34. Audran, G.; Marque, S. R. A.; Mellet, P. *Acc. Chem. Res.* **2020,** *53,* 2828–2840. doi:10.1021/acs.accounts.0c00457
35. Hirsch, M.; Hofmann, L.; Yakobov, I.; Kahremany, S.; Sameach, H.; Shenberger, Y.; Gevorkyan-Airapetov, L.; Ruthstein, S. *Biophys. Rep.* **2024,** *4,* 100168. doi:10.1016/j.bpr.2024.100168
36. Shu, C.; Yang, Z.; Rajca, A. *Chem. Rev.* **2023,** *123,* 11954–12003. doi:10.1021/acs.chemrev.3c00406
37. Torricella, F.; Pierro, A.; Mileo, E.; Belle, V.; Bonucci, A. *Biochim. Biophys. Acta, Proteins Proteomics* **2021,** *1869,* 140653. doi:10.1016/j.bbapap.2021.140653
38. Xu, Y.; Teng, C.; Wang, Y.; Chen, D.; Yin, D.; Yan, L. *J. Colloid Interface Sci.* **2024,** *669,* 578–589. doi:10.1016/j.jcis.2024.05.032
39. Barré, R.; Mouchel dit Leguerrier, D.; Fedele, L.; Imbert, D.; Molloy, J. K.; Thomas, F. *Chem. Commun.* **2020,** *56,* 435–438. doi:10.1039/c9cc06524e
40. Huang, S.; Xu, M.; Da, Q.; Jing, L.; Wang, H. *Cancers* **2024,** *16,* 351. doi:10.3390/cancers16020351
41. Liang, J.; Zhang, P.; Yang, H.; Zhang, Y.; Yao, T.; Liu, K.; Wang, Y.; Zhang, X.; Qin, X. *Eur. J. Med. Chem.* **2022,** *236,* 114331. doi:10.1016/j.ejmech.2022.114331
42. Kirilyuk, I. A.; Svyatchenko, V. A.; Morozov, D. A.; Kazachinskaya, E. I.; Kiselev, N. N.; Bakunova, S. M.; Voinov, M. A.; Loktev, V. B.; Grigoryev, I. A. *Antibiot. Chemother. (Moscow, Russ. Fed.)* **2012,** *57,* 3–12.
43. Ali, B. M.; Velavan, B.; Sudhandiran, G.; Sridevi, J.; Nasar, A. S. *Eur. Polym. J.* **2020,** *122,* 109354. doi:10.1016/j.eurpolymj.2019.109354
44. Tretyakov, E.; Gorbunov, D.; Gritsan, N.; Keerthi, A.; Baumgarten, M.; Schollmeyer, D.; Ivanov, M.; Sergeeva, A.; Fedin, M. *RSC Adv.* **2024,** *14,* 6178–6189. doi:10.1039/d4ra00916a
45. Mutlu, H. *Polym. Chem.* **2022,** *13,* 1648–1657. doi:10.1039/d1py01645h
46. Benny, A. T.; Arikkatt, D. S.; Vazhappilly, C. G.; Kannadasan, S.; Thomas, R.; Leelabaiamma, M. S. N.; Radhakrishnan, E. K.; Shanmugam, P. *Mini-Rev. Med. Chem.* **2022,** *22,* 1030–1063. doi:10.2174/1389557521666211124141859
47. Vavsari, V. F.; Balalaie, S. *Chem. Heterocycl. Compd.* **2020,** *56,* 404–407. doi:10.1007/s10593-020-02675-8
48. Maicheen, C.; Churnthammakarn, C.; Pongsroypech, N.; Khamkhenshorngphanuch, T.; Ungwitayatorn, J.; Rungsardthong, K.; Asasutjarit, R.; Theeramunkong, S. *Molecules* **2023,** *28,* 3129. doi:10.3390/molecules28073129
49. Mao, L.-L.; Liu, Y.; Wan, J.-P. *Chin. Chem. Lett.* **2025,** *36,* 110784. doi:10.1016/j.cclet.2024.110784
50. Huffman, K. R.; Kuhn, C. E.; Zweig, A. *J. Am. Chem. Soc.* **1970,** *92,* 599–605. doi:10.1021/ja00706a030
51. Agliulin, K. V.; Stepanov, A. V.; Yarovenko, V. N.; Krayushkin, M. M.; Tretyakov, E. V.; Nasyrova, D. I.; Ilyushenkova, V. V.; Ayt, A. O.; Valova, T. M. *Mendeleev Commun.* **2024,** *34,* 828–830. doi:10.1016/j.mencom.2024.10.019
52. Agliulin, K. V.; Stepanov, A. V.; Yarovenko, V. N.; Krayushkin, M. M.; Tretyakov, E. V.; Ayt, A. O.; Valova, T. M. *Mendeleev Commun.*, in press.
53. Levchenko, K. S.; Barachevski, V. A.; Yarovenko, V. N.; Krayushkin, M. M.; Semenova, I. S.; Kobeleva, O. I.; Valova, T. M.; Shmelin, P. S. *Chem. Heterocycl. Compd.* **2011,** *47,* 155–165. doi:10.1007/s10593-011-0736-x
54. Semenova, I. S.; Levchenko, K. S.; Yarovenko, V. N.; Krayushkin, M. M.; Barachevskii, V. A.; Kobeleva, O. I.; Valova, T. M. *Russ. Chem. Bull.* **2012,** *61,* 1761–1768. doi:10.1007/s11172-012-0242-z
55. Krayushkin, M. M.; Yarovenko, V. N. *Russ. Chem. Bull.* **2026,** *75,* 1046–1061. doi:10.1007/s11172-026-4957-7
56. Kobeleva, O. I.; Valova, T. M.; Barachevsky, V. A.; Semenova, I. S.; Levchenko, K. S.; Yarovenko, V. N.; Krayushkin, M. M. *Opt. Spectrosc.* **2013,** *114,* 401–405. doi:10.1134/s0030400x13020112
57. Barachevsky, V. A.; Kobeleva, O. I.; Valova, T. M.; Ait, A. O.; Dunaev, A. A.; Gorelik, A. M.; Krayushkin, M. M.; Levchenko, K. S.; Yarovenko, V. N.; Kiyko, V. V.; Grebennikov, E. P. *Opt. Mem. Neural Network* **2010,** *19,* 187–195. doi:10.3103/s1060992x10020104
58. D'Auria, M. *J. Org. Chem.* **2000,** *65,* 2494–2498. doi:10.1021/jo991655p
59. Cummings, R. T.; DiZio, J. P.; Krafft, G. A. *Tetrahedron Lett.* **1988,** *29,* 69–72. doi:10.1016/0040-4039(88)80018-2
60. D'Auria, M.; D'Onofrio, F.; Vantaggi, A. *Tetrahedron* **1990,** *46,* 7831–7840. doi:10.1016/s0040-4020(01)90080-8
61. D'Auria, M.; D'Annibale, A.; Ferri, T. *Tetrahedron* **1992,** *48,* 9323–9336. doi:10.1016/s0040-4020(01)85622-2
62. Gagarskiy, S. V.; Grebennikov, E. P.; Kiyko, V. V.; Levchenko, K. S.; Sergeev, A. N.; Fomicheva, Y. Y.; Oberhofer, K.; Iglev, H. *Opt. Spectrosc.* **2018,** *125,* 482–486. doi:10.1134/s0030400x18100089
63. Fomicheva, Y. Y. Transformation of chromone based organic compounds under single-photon and multiphoton laser excitation. Ph.D. Thesis, ITMO University, Saint Petersburg, 2020. https://search.rsl.ru/ru/record/01010645662
64. Agliulin, K. V.; Stepanov, A. V.; Nasyrova, D. I.; Ilyushenkova, V. V.; Yarovenko, V. N.; Krayushkin, M. M.; Ayt, A. O.; Tretyakov, E. V. *Asian J. Org. Chem.* **2026,** *15,* e70454. doi:10.1002/ajoc.70454

65. Tope, S. In *Verified Market Reports. Global Optical Disc Market Size, Share, Growth Trends & Industry Forecast 2026–2034,* 7th ed.; Turner, C., Ed.; 2026. https://www.verifiedmarketreports.com/product/optical-disc-market/
66. Zhao, M.; Wen, J.; Hu, Q.; Wei, X.; Zhong, Y.-W.; Ruan, H.; Gu, M. *Nature* **2024,** *626,* 772–778. doi:10.1038/s41586-023-06980-y
67. Jain, A.; Rahimian, M. G.; Bhardwaj, V. R. *Photonics* **2022,** *9,* 690. doi:10.3390/photonics9100690
68. Ma, T.; Ma, M.; Guo, L. J. *iScience* **2025,** *28,* 112222. doi:10.1016/j.isci.2025.112222
69. Wang, M. M.; Esener, S. C.; McCormick, F. B.; Çokgör, I.; Dvornikov, A. S.; Rentzepis, P. M. *Opt. Lett.* **1997,** *22,* 558–560. doi:10.1364/ol.22.000558
70. Hunter, S.; Kiamilev, F.; Esener, S.; Parthenopoulos, D. A.; Rentzepis, P. M. *Appl. Opt.* **1990,** *29,* 2058–2066. doi:10.1364/ao.29.002058
71. Dvornikov, A. S.; Walker, E. P.; Rentzepis, P. M. *J. Phys. Chem. A* **2009,** *113,* 13633–13644. doi:10.1021/jp905655z
72. Walker, E.; Dvornikov, A.; Coblentz, K.; Esener, S.; Rentzepis, P. *Opt. Express* **2007,** *15,* 12264–12276. doi:10.1364/oe.15.012264
73. Walker, E.; Rentzepis, P. M. *Nat. Photonics* **2008,** *2,* 406–408. doi:10.1038/nphoton.2008.121
74. Kiyko, V. V. Multi-layer optical disc. U.S. Patent 8455079, June 4, 2013.
75. Ayt, A. O.; Barachevsky, V. A.; Duensing, A.; Fomicheva, Y. Y.; Gagarskiy, S. V.; Iglev, H.; Kiyko, V. V.; Krayushkin, M. M.; Sergeev, A. N.; Veniaminov, A. V.; Zakharov, V. V. *Opt. Quantum Electron.* **2017,** *49,* 72. doi:10.1007/s11082-017-0900-3
76. Chen, Z. X.; Li, Y.; Huang, F. *Chem* **2021,** *7,* 288–332. doi:10.1016/j.chempr.2020.09.024
77. Mizuno, A.; Matsuoka, R.; Mibu, T.; Kusamoto, T. *Chem. Rev.* **2024,** *124,* 1034–1121. doi:10.1021/acs.chemrev.3c00613
78. Kimura, S.; Kimura, S.; Kato, K.; Teki, Y.; Nishihara, H.; Kusamoto, T. *Chem. Sci.* **2021,** *12,* 2025–2029. doi:10.1039/d0sc05965j
79. Xie, G.; Xiao, D.; Yang, Q.; Ye, T.; Chen, R.; Huang, W. Luminescent organic radicals toward breakthrough of organic optoelectronics. In *Organic Radicals;* Wang, C.; Labidi, A.; Lichtfouse, E., Eds.; Elsevier, 2024; pp 183–209. doi:10.1016/b978-0-443-13346-6.00006-3
80. Blinco, J. P.; Fairfull-Smith, K. E.; Morrow, B. J.; Bottle, S. E. *Aust. J. Chem.* **2011,** *64,* 373–389. doi:10.1071/ch10442
81. Tretyakov, E. V.; Plyusnin, V. F.; Suvorova, A. O.; Larionov, S. V.; Popov, S. A.; Antonova, O. V.; Zueva, E. M.; Stass, D. V.; Bogomyakov, A. S.; Romanenko, G. V.; Ovcharenko, V. I. *J. Lumin.* **2014,** *148,* 33–38. doi:10.1016/j.jlumin.2013.11.017
82. Likhtenstein, G. I.; Ishii, K.; Nakatsuji, S. *Photochem. Photobiol.* **2007,** *83,* 871–881. doi:10.1111/j.1751-1097.2007.00141.x
83. Cho, E.; Coropceanu, V.; Brédas, J.-L. *J. Mater. Chem. C* **2021,** *9,* 10794–10801. doi:10.1039/d1tc01702k
84. Guo, J.; Abdinejad, M.; Farzi, A.; Salehi, M.; Seifitokaldani, A. *Energy Adv.* **2023,** *2,* 877–885. doi:10.1039/d3ya00108c
85. Gwozdzinski, K.; Pieniazek, A.; Gwozdzinski, L. *Molecules* **2025,** *30,* 2159. doi:10.3390/molecules30102159
86. DeJulius, C. R.; Dollinger, B. R.; Kavanaugh, T. E.; Dailing, E.; Yu, F.; Gulati, S.; Miskalis, A.; Zhang, C.; Uddin, J.; Dikalov, S.; Duvall, C. L. *Bioconjugate Chem.* **2021,** *32,* 928–941. doi:10.1021/acs.bioconjchem.1c00081
87. Imoto, T.; Matsumoto, H.; Nonaka, S.; Shichijo, K.; Nagao, M.; Shimakoshi, H.; Hoshino, Y.; Miura, Y. *Polymers (Basel, Switz.)* **2022,** *14,* 5123. doi:10.3390/polym14235123
88. Alberti, D.; Thiaudiere, E.; Parzy, E.; Elkhanoufi, S.; Rakhshan, S.; Stefania, R.; Massot, P.; Mellet, P.; Aime, S.; Geninatti Crich, S. *Sci. Rep.* **2023,** *13,* 13725. doi:10.1038/s41598-023-40857-4
89. Gilan, M. M.; Habibi, D. *Sci. Rep.* **2025,** *15,* 22554. doi:10.1038/s41598-025-06368-0
90. Gorini, L.; Caneschi, A.; Menichetti, S. *Synlett* **2006,** 948–950. doi:10.1055/s-2006-939045
91. Zayakin, I. A.; Zimina, A. M.; Tretyakov, E. V. *Russ. J. Org. Chem.* **2025,** *61,* 1011–1033. doi:10.1134/s1070428025601608
92. Zayakin, I. A.; Romanenko, G. V.; Korlyukov, A. A.; Tretyakov, E. V. *Organometallics* **2025,** *44,* 892–898. doi:10.1021/acs.organomet.5c00042
93. Agliulin, K. V.; Stepanov, A. V.; Zayakin, I. A.; Yarovenko, V. N.; Krayushkin, M. M.; Tretyakov, E. V.; Nasyrova, D. I.; Ayt, A. O.; Valova, T. M. *Russ. Chem. Bull.* **2024,** *73,* 3342–3351. doi:10.1007/s11172-024-4450-0
94. McConnell, H. M. *J. Chem. Phys.* **1963,** *39,* 1910. doi:10.1063/1.1734562
95. Romanov, V.; Bagryanskaya, I.; Gritsan, N.; Gorbunov, D.; Vlasenko, Y.; Yusubov, M.; Zaytseva, E.; Luneau, D.; Tretyakov, E. *Crystals* **2019,** *9,* 219. doi:10.3390/cryst9040219
96. Tretyakov, E.; Fedyushin, P.; Bakuleva, N.; Korlyukov, A.; Dorovatovskii, P.; Gritsan, N.; Dmitriev, A.; Akyeva, A.; Syroeshkin, M.; Stass, D.; Zykin, M.; Efimov, N.; Luneau, D. *J. Org. Chem.* **2023,** *88,* 10355–10370. doi:10.1021/acs.joc.2c01793
97. Tretyakov, E.; Okada, K.; Suzuki, S.; Baumgarten, M.; Romanenko, G.; Bogomyakov, A.; Ovcharenko, V. *J. Phys. Org. Chem.* **2016,** *29,* 725–734. doi:10.1002/poc.3561
98. Johnston, L. J.; Tencer, M.; Scaiano, J. C. *J. Org. Chem.* **1986,** *51,* 2806–2808. doi:10.1021/jo00364a036

License and Terms

This is an open access article licensed under the terms of the Beilstein-Institut Open Access License Agreement (https://www.beilstein-journals.org/bjoc/terms), which is identical to the Creative Commons Attribution 4.0 International License (https://creativecommons.org/licenses/by/4.0). The reuse of material under this license requires that the author(s), source and license are credited. Third-party material in this article could be subject to other licenses (typically indicated in the credit line), and in this case, users are required to obtain permission from the license holder to reuse the material.

The definitive version of this article is the electronic one which can be found at: https://doi.org/10.3762/bjoc.22.137